

# A Precision-Positioning Method for a High-Acceleration Low-Load Mechanism Based on Optimal Spatial and Temporal Distribution of Inertial Energy

Xin Chen, Youdun Bai, Zhijun Yang\*, Jian Gao, Gongfa Chen

**ABSTRACT** High-speed and precision positioning are fundamental requirements for high-acceleration low-load mechanisms in integrated circuit (IC) packaging equipment. In this paper, we derive the transient nonlinear dynamic-response equations of high-acceleration mechanisms, which reveal that stiffness, frequency, damping, and driving frequency are the primary factors. Therefore, we propose a new structural optimization and velocity-planning method for the precision positioning of a high-acceleration mechanism based on optimal spatial and temporal distribution of inertial energy. For structural optimization, we first reviewed the commonly flexible multibody dynamic optimization using equivalent static loads method (ESLM), and then we selected the modified ESLM for optimal spatial distribution of inertial energy; hence, not only the stiffness but also the inertia and frequency of the real modal shapes are considered. For velocity planning, we developed a new velocity-planning method based on nonlinear dynamic-response optimization with varying motion conditions. Our method was verified on a high-acceleration die bonder. The amplitude of residual vibration could be decreased by more than 20% via structural optimization and the positioning time could be reduced by more than 40% via asymmetric variable velocity planning. This method provides an effective theoretical support for the precision positioning of high-acceleration low-load mechanisms.

**KEYWORDS** high-acceleration low-load mechanism, precision positioning, spatial and temporal distribution, inertial energy, equivalent static loads method (ESLM), velocity planning

## 1 Introduction

With the rapid development of electronic manufacturing technology and the electronic market, the demand for high-

acceleration and high-precision mechanisms are increasing. For example, some manipulators in packaging equipment run at the speed of 20 000–24 000 cycle times per hour, with peak acceleration of 12g–15g and a positioning precision of 2–5  $\mu\text{m}$ . High-acceleration and short-cycling-time mechanisms are inevitably subjected to elastic deformation and vibrations caused by the inertial force. It is very difficult to achieve high positioning accuracy in a very short deceleration phase. Frequent but short acceleration-deceleration cycles could result in abrasion or even failure of the mechanisms [1]. Hence, it is necessary to find a new approach to optimize this type of mechanism.

When a mechanism moves at high speed, its components should be regarded as flexible bodies, so the whole mechanism becomes a flexible multibody dynamic system, in which the rigid-body motion is coupled with the elastic deformation. Therefore, the resulting dynamic model is a set of high-dimensional differential equations with time-varying coefficients and non-smooth nonlinear terms, which is difficult to model, analyze, and optimize [2]. For the last two decades, though tremendous progress has been achieved in the analysis of kinematics and the dynamics of flexible multibody dynamic systems [3], the optimization of flexible multibody dynamic systems is not completely solved.

The equivalent static loads method (ESLM) [4–10] proposed by Park et al. is the most effective method for the dynamic optimization of flexible multibody dynamic systems. It has been implemented into the commercial software HyperWorks. The ESLM has been successfully used in the optimization of automotive collision dynamics, Boeing aircraft wing structure [9], and so forth. The main idea of this method is to convert the nonlinear dynamic response, by discretizing the time variable, into response equations of a series of equivalent static loads [4–10]. As the current dynamic topology optimization methods only consider some natural frequencies, but the corresponding mode shapes may not reflect the real deforma-

The Key Laboratory of Mechanical Equipment Manufacturing & Control Technology of Ministry of Education, Guangdong University of Technology, Guangzhou 510006, China

\* Correspondence author. E-mail: yangzj@gdut.edu.cn

Received 4 January 2015; received in revised form 16 June 2015; accepted 30 June 2015

tion. Another important factor is the motion profile. At present, velocity-planning methods mainly consider geometric smoothing while ignoring the influence of curve parameters on the dynamic response. The S curve has a smoother variation in acceleration compared to the trapezoidal profile, so it can reduce the residual vibration to some extent [11, 12]. Input shaping, such as a digital filter, not only causes time delay, but also is difficult to apply to the nonlinear dynamic system, where both stiffness and frequencies vary with position [13]. Therefore, a dynamic-response optimization for the velocity planning is necessary. Some scholars have an equivalent motion stage system as a single-degree-of-freedom system to obtain optimal parameters of the S-type motion curve to reduce residual vibration [14]. However, because of high-acceleration low-load mechanism is three dimensional and frequently starts and stops, its velocity planning is a much more complicated problem.

In this paper, the nonlinear dynamic response of a high-acceleration low-load mechanism is discussed. We derive the transient nonlinear dynamic-response equations of high acceleration mechanisms, which reveal that stiffness, frequencies, and damping (related to the layout of material, i.e., the spatial distribution of inertial energy), as well as the driving frequency (related to the motion profile, i.e., the temporal distribution of inertial energy), are the primary factors. Therefore, we propose a new structural optimization and velocity-planning method for the precision positioning of a high acceleration mechanism based on optimal spatial and temporal distribution of inertial energy. For structural optimization, the ESLM-based flexible multibody dynamic optimization is reviewed and modified for high-acceleration low-load mechanisms by means of the Rayleigh-Ritz method, which has been done in our previous work [15, 16]. For velocity planning, a new asymmetric velocity profile is proposed based on nonlinear dynamic optimization with varying boundary conditions. Finally, a practical example of a high-speed die bonder is studied, which shows that the residual vibration can be reduced by more than 20% by structural optimization and the positioning time can be reduced by more than 40% by asymmetric variable velocity planning. Numerical tests show that the proposed method is efficient for structural design and velocity planning for a high-acceleration low-load mechanism.

## 2 Technical background

For mechanisms operating at very high speed, the vibration of the structures must be considered. When the deformation is large, the absolute nodal coordinate formulation (ANCF) is more efficient [16]. Within the ANCF for highly flexible bodies, the absolute coordinates are represented by a vector  $y$ , characterizing the material points of the bodies by an appropriate shape function. The motion equation is

$$M(t)\dot{y} + C(t)\dot{y} + K(t)y = q(t) \quad (1)$$

where  $M(t)$ ,  $C(t)$  and  $K(t)$  are mass, damping, and stiffness matrices at time  $t$ , respectively. The motion equation for flexible bodies has the same format as that of structural vibration.

The displacement  $y$  consists of rigid motion  $y_R$  and elastic modes  $y_E$ . If we consider when the mechanism moves at a position, the mechanism can be regarded as a structure with kinetic degrees of freedom. Let  $u_R$  and  $u_E$  be the displacements of the rigid modes and elastic modes, respectively. Therefore, the total displacement of the flexible multibody is

$$u(t) = u_R(t) + u_E(t) = \Phi_R \eta_R(t) + \Phi_E \eta_E(t) \quad (2)$$

where  $\Phi_R$  and  $\Phi_E$  are the matrices of the modal shapes of the rigid modes and elastic modes; and  $\eta_R$  and  $\eta_E$  are the corresponding coordinates. The modal shape of the whole system is the combination of  $\Phi_R$  and  $\Phi_E$ :

$$\Phi = [\Phi_R \quad \Phi_E] \quad (3)$$

For the rigid modes, there exists

$$M_R \ddot{\eta}_R = \Phi_R^T q(t) \quad (4)$$

And for the elastic modes, the following equation is satisfied:

$$M_E \ddot{\eta}_E + C_E \dot{\eta}_E + K_E \eta_E = \Phi_E^T q(t) \quad (5)$$

where  $M_R = \Phi_R^T M \Phi_R$  denotes the modal mass of the rigid modes;  $M_E = \Phi_E^T M \Phi_E$ ,  $C_E = \Phi_E^T C \Phi_E$ ,  $K_E = \Phi_E^T K \Phi_E = M_E \Lambda_E$  are the modal mass, modal damping, and modal stiffness of the elastic modes, respectively; and  $\Phi_R^T q(t)$  is the modal load. Assuming that  $C_E = \Phi_E^T C \Phi_E = M_E \Gamma_E$ , the eigenvalues of the damped elastic modes are

$$\Gamma_E = \begin{bmatrix} 2\xi_{E1}\omega_{E1} & & & \\ & 2\xi_{E2}\omega_{E2} & & \\ & & \ddots & \\ & & & 2\xi_{En}\omega_{En} \end{bmatrix} \quad (6)$$

For each degree of freedom:

$$\ddot{\eta}_{Ei} + 2\xi_{Ei}\omega_{Ei}\dot{\eta}_{Ei} + \omega_{Ei}^2\eta_{Ei} = \frac{1}{m_{Ei}}q_{Ei}(t) \quad (7)$$

where  $\xi_{Ei} = \frac{c_{Ei}}{2m_{Ei}\omega_{Ei}}$ , Eq. (7) is similar to the dynamic response of a one-degree-of-freedom system.

Assume that the input force is a harmonic excitation:

$$q_E(t) = F_E \cos(\Omega t) \quad (8)$$

Using modal superposition and assuming that  $n$  modes are considered, the modal velocity is

$$\dot{\eta}_{Ei}(t) = \sum_{i=1}^n -\Omega \frac{F_E/K_{Ei}}{\sqrt{(1-\bar{\omega}_{Ei}^2)^2 + (2\xi_{Ei}\bar{\omega}_{Ei})^2}} \sin(\Omega t + \phi_{Hi}) \quad (9)$$

where

$$\tan(\phi_{Hi}) = \frac{2\xi_{Ei}\bar{\omega}_{Ei}}{1-\bar{\omega}_{Ei}^2}, \quad \bar{\omega}_{Ei} = \frac{\Omega}{\omega_{Ei}} \quad (10)$$

Usually, if we transfer the high-speed motion profile to the frequency domain using a fast Fourier transformation (Figure 1), the input force can be regarded as a series of harmonic excitations:

$$q_E(t) = \sum_{j=1}^m F_{Ej} \cos(\Omega_j t) \quad (11)$$

So the corresponding modal velocity should be

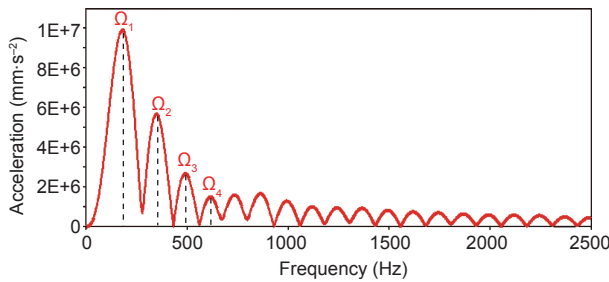


Figure 1. The series of harmonic motions in the frequency domain.

$$\dot{q}_{Ei}(t) = \sum_{j=1}^m \sum_{i=1}^n -\Omega_j \frac{F_{Eij}/K_{Eij}}{\sqrt{(1-\bar{\omega}_{Eij}^2)^2 + (2\zeta_{Eij}\omega_{Eij})^2}} \sin(\Omega_j t + \phi_{Hi}) \quad (12)$$

Eq. (12) shows that the vibration response of the high-speed mechanism is affected by the stiffness, damping, and frequencies of elastic modes, and also by the excitation frequencies. The former is related to the structural design and the latter is related to the motion profile, so the optimal spatial and temporal distribution of inertial energy would be an efficient way to minimize the vibration at the end of the manipulator and the final stage of the motion.

However, as the vibration response is difficult to obtain due to the variation in stiffness, inertia, and motion conditions, numerical methods such as the nonlinear finite element method of flexible multibody dynamics are needed to solve the dynamic-response analysis and optimization.

### 3 Optimal structural design using ESLM

The motion equation for an equivalent structural response under a dynamic load at position  $y_R$  can be written as

$$M(y_R)\ddot{y}_E + K(y_R)y_E = q(y_R, t) \quad (13)$$

where vectors  $y_R$  and  $y_E$  represent the displacement of the rigid body and elastic deformation, respectively, and the damping effect is ignored.

With the ESLM [10], we can derive the equivalent static loads using the finite element method. Rearranging Eq. (13) leads to

$$K(y_R)y_E = q(y_R, t) - M(y_R)\ddot{y}_E \quad (14)$$

or

$$K(y_R)y_E = f_{eq} \quad (15)$$

$$f_{eq} = q(y_R, t) - M(y_R)\ddot{y}_E \quad (16)$$

where Eq. (16) represents the equivalent static loads at time  $t$  [10].

For optimization, the number of the equivalent static loads (Figure 2) can be treated as multiple loading conditions. Thus, the equivalent load set can regenerate dynamic properties such as time-dependent displacement or stress.

In fact, the ESLM is an interface between nonlinear response analysis and linear static optimization (Figure 3), and analysis is performed in the analysis domain, where equivalent loads are calculated. Linear-response optimization is performed using the equivalent static loads in the design domain. The process proceeds in a cyclic manner.

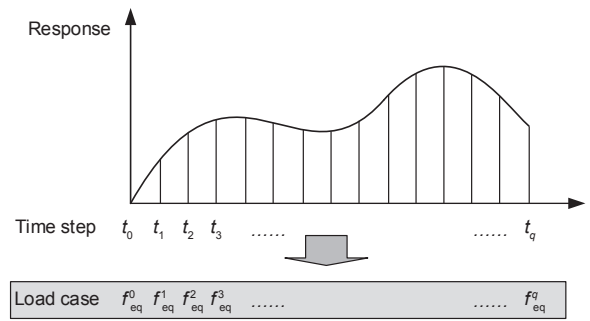


Figure 2. Equivalent static loads in the number of time points.

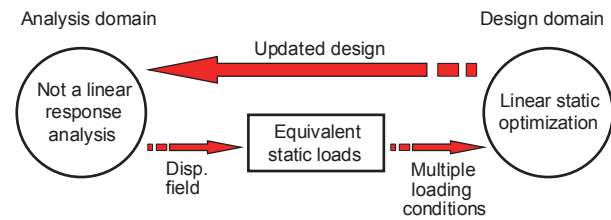


Figure 3. The analysis and design domain using the ESLM.

In high-acceleration low-load mechanisms, the principal loads are the inertial forces induced by accelerations. Hence, mechanical design should consider light-weight structures to minimize such loads. However, the linear static optimization cannot handle dynamic features such as inertial property and dynamic stiffness, even within the ESLM. Linear static optimization needs to be modified with only one iteration can be reflected on the inertial forces. Moreover, we have to modify the sensitivity analysis of the ESLM to meet the requirements of a high-acceleration low-load mechanism.

### 4 A new structural-design method based on optimal spatial distribution of inertial energy

In the original ESLM, only the stiffness changes are considered when removing an element, so the element sensitivity is defined by the element strain energy [10, 15]. However, the modification of elements also changes the inertial force, resulting in a change to the strain energy [16]. Assuming that the  $i$ th element is removed from the reference structure at the  $j$ th position, the change in strain energy is

$$\begin{aligned} \Delta E_{i,j}^S &= \frac{1}{2} f_j^T \Delta y_{i,j} = \frac{1}{2} (y_j^T K_j^T) K_j^{-1} (\Delta K_{i,j} y_j + \Delta M_{i,j} \ddot{y}_j) \\ &= \frac{1}{2} y_j^T \Delta K_{i,j} y_j + \frac{1}{2} y_j^T \Delta M_{i,j} \ddot{y}_j \\ &= \frac{1}{2} y_j^T K_{i,j}^e y_j + \frac{1}{2} y_j^T M_{i,j}^e \ddot{y}_j \end{aligned} \quad (17)$$

where superscripts T, e, and S refer to transposition, element, and strain, respectively;  $\Delta$  is the increment; and  $E$  is energy.

In addition, in a high-acceleration low-load mechanism, the inertial force is the main load, so the inertial property should be considered. Like the strain energy, the inertial property can be measured by the kinetic energy. Accordingly, when an

element  $i$  is removed from the reference structure at position  $j$ , the change in kinematic energy is

$$\Delta E_{i,j}^K = -\frac{1}{2}m_i(r_{i,j}\omega_j)^2 = -\frac{1}{2}m_i\dot{y}_{i,j}^2 \quad (18)$$

where the superscript K means kinematic;  $m_i$  is the mass of the  $i$ th element;  $\omega_j$  is the rotational velocity at the  $j$ th position; and  $r_{i,j}$  and  $\dot{y}_{i,j}$  are the gyro radius and velocity of the center of the  $i$ th element in the  $j$ th position, respectively.

For high-acceleration mechanisms, we need to maximize the stiffness while minimizing the inertia. As with the Rayleigh-Ritz analysis, we can divide the strain energy by the kinematic energy to quantify the sensitivity of an element:

$$\Delta S_{i,j} = \frac{\Delta E_{i,j}^S}{\Delta E_{i,j}^K} = \frac{\frac{1}{2}\mathbf{y}_j^T \mathbf{K}_{i,j}^e \mathbf{y}_j + \frac{1}{2}\mathbf{y}_j^T \mathbf{M}_{i,j}^e \ddot{\mathbf{y}}_j}{\frac{1}{2}m_i\dot{y}_j^2} \quad (19)$$

Assuming that the number of discrete positions is  $m$ , and that  $\Delta S_{\max,j}$  is the maximum sensitivity at the  $j$ th position, the comprehensive sensitivity is defined by

$$\Delta S_i = \frac{1}{m} \sum_{j=1}^m \frac{\Delta S_{i,j}}{\Delta S_{\max,j}} \quad (20)$$

Evolution structural optimization (ESO) is employed to perform the modification. If the  $\Delta S_i$  is less than a given threshold, the material property is set as a deleted material density, the elastic modulus of which is very low, only 1%–10% of that of the normal material.

If we normalize the total  $E_s$  by the scalar product of displacement and the total  $E_K$  by the scalar product of velocity, we form the  $\tilde{E}_s$  and  $\tilde{E}_K$ , respectively. Then the ratio of  $\tilde{E}_s$  to  $\tilde{E}_K$  should reach a maximum regardless of the deformation and speed:

$$S = \frac{\tilde{E}_s}{\tilde{E}_K} = \frac{E_s / (\frac{1}{2}\mathbf{y}^T \mathbf{y})}{E_K / (\frac{1}{2}\dot{\mathbf{y}}^T \dot{\mathbf{y}})} = \frac{\frac{1}{2}\mathbf{y}^T \mathbf{K} \mathbf{y} / (\frac{1}{2}\mathbf{y}^T \mathbf{y})}{\frac{1}{2}\dot{\mathbf{y}}^T \mathbf{M} \dot{\mathbf{y}} / (\frac{1}{2}\dot{\mathbf{y}}^T \dot{\mathbf{y}})} \quad (21)$$

The optimization problem of high-acceleration low-load mechanisms becomes

$$\begin{aligned} & \text{Max } S \\ & \text{s.t. } U \leq U^* \end{aligned} \quad (22)$$

where  $U$  is the residual vibration amplitude within a required stationary time and  $U^*$  is the positioning precision requirement.

We made a stand-alone program for sensitivity analysis and generated the command to modify the model. It can be integrated with the commercial software I-DEAS and ADAMS to perform an optimization design for a high acceleration mechanism.

### 5 Motion profile based on temporal optimal distribution of inertial energy

As high-acceleration low-load mechanisms start and stop frequently, the primary motion-control policy is open-loop control with a prescribed motion profile, and the performance is mainly dependent on the parameter of the given motion

curve. As we can see in Section 2, the motion profile can be transformed to a series of harmonic excitations in the frequency domain, which causes difficulty in calculations of the nonlinear dynamic response. However, if we can parameterize the motion profile as variable motion boundary conditions, we can achieve optimum parameters for the motion profile using nonlinear dynamic-response optimization. In particular, when the machine moves at very high speed, such as during die bonding and wire bonding, the input signal consists of pulses or jumps with sudden changes. Since the S curve is widely used in industrial situations, we take the asymmetric S curve as an example. The parameters are four jerks for each section (Figure 4), namely  $G_1$ – $G_4$ .

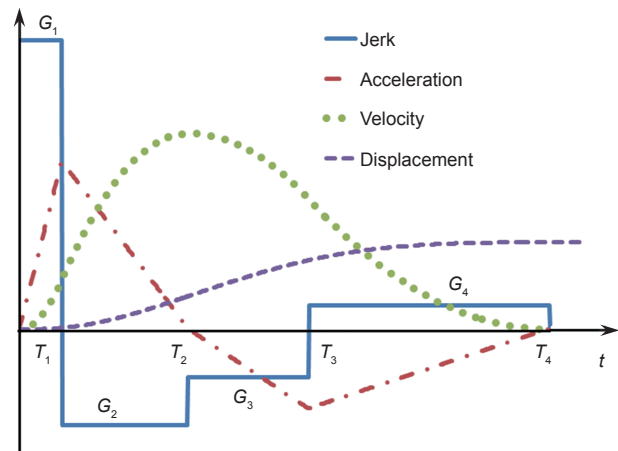


Figure 4. The parameters of the asymmetric S curve.

The optimization model can be described as

$$\begin{aligned} & T = T_1 + T_2 + T_3 + T_4 + T_s \\ & \text{Find}(G_1, G_2, G_3, G_4). \\ & \text{Objective: Min}(T) \\ & \text{Subject to: } \text{abs}(s - s^*) + \text{abs}(v) < \varepsilon \quad (23) \\ & T_1 G_1 = T_2 G_2 \\ & T_3 G_3 = T_4 G_4 \\ & T_1 G_1 (T_1 + T_2) = T_3 G_3 (T_3 + T_4) \end{aligned}$$

The following equation is used to determine when the positioning accuracy is reached:

$$\text{abs}(s - s^*) + \text{abs}(v) < \varepsilon \quad (24)$$

Let the objective position  $s^*$  be  $Q$ . Then the time segment for each motion is

$$T_1 = \sqrt[3]{\frac{\sqrt[3]{6} E (F + G + H + I + J)^2}{G_1 (A + B + C + D)}} \quad (25)$$

$$T_2 = \frac{G_1 T_1}{G_2} \quad (26)$$

$$T_3 = T_1 \sqrt{\frac{G_1 (1 + \frac{G_1}{G_2})}{G_3 (1 + \frac{G_3}{G_4})}} \quad (27)$$

$$T_4 = \frac{T_3 G_3}{G_4} \quad (28)$$

where

$$\begin{aligned} A &= 2G_1^2 G_3^2 G_4 + 2G_1^2 G_3 G_4^2 + 3G_1 G_2 G_3^2 G_4 \\ &\quad + 3G_1 G_2 G_3 G_4^2 + G_2^2 G_3^2 G_4 + G_2^2 G_3 G_4^2 \\ B &= G_1 G_3 \sqrt{G_2 G_3 (G_3 + G_4)} G_1 G_4 (G_1 + G_2) \\ &\quad + 2G_1 G_4 \sqrt{G_2 G_3 (G_3 + G_4)} G_1 G_4 (G_1 + G_2) \\ C &= G_2 G_3 \sqrt{G_2 G_3 (G_3 + G_4)} G_1 G_4 (G_1 + G_2) \\ D &= 2G_2 G_4 \sqrt{G_2 G_3 (G_3 + G_4)} G_1 G_4 (G_1 + G_2) \\ E &= Q G_2^2 G_3 G_4 (G_3 + G_4) G_1^2 \\ F &= 2G_1^2 G_3^2 G_4 + 2G_1^2 G_3 G_4^2 + 3G_1 G_2 G_3^2 G_4 \\ &\quad + 3G_1 G_2 G_3 G_4^2 + G_2^2 G_3^2 G_4 + G_2^2 G_3 G_4^2 \\ G &= G_1 G_3 \sqrt{G_2 G_3 (G_3 + G_4)} G_1 G_4 (G_1 + G_2) \\ H &= 2G_1 G_4 \sqrt{G_2 G_3 (G_3 + G_4)} G_1 G_4 (G_1 + G_2) \\ I &= G_2 G_3 \sqrt{G_2 G_3 (G_3 + G_4)} G_1 G_4 (G_1 + G_2) \\ J &= 2G_2 G_4 \sqrt{G_2 G_3 (G_3 + G_4)} G_1 G_4 (G_1 + G_2) \end{aligned}$$

Using the variable motion boundary condition nonlinear dynamic-optimization method, the procedure is shown as follows:

- (1) Define the design variables,  $G_1$ ,  $G_2$ ,  $G_3$ ,  $G_4$ , and the position objective  $Q$ . Define the time variables  $T_1$ ,  $T_2$ ,  $T_3$ ,  $T_4$ , and evaluate them using Eqs. (25)–(28), respectively. Define the time interval  $T_{12} = T_1 + T_2$ ,  $T_{123} = T_{12} + T_3$ , and  $T_{1234} = T_{123} + T_4$ .
- (2) Build the geometry of the mechanism, assign materials, build joints, and apply motion, using the following function:
 
$$\text{IF}(T < T_1: G_1, -G_2, \text{IF}(T < T_{12}: -G_2, G_3, \text{IF}(T < T_{123}: G_3, -G_4, \text{IF}(T < T_{1234}: -G_4, 0, 0)))$$
- (3) Mesh the key parts, assign element properties, and create the degrees of freedom of the connection; define the solution type as super element creation, and solve and output the modal neutral file.
- (4) Replace the rigid body with the corresponding flexible multibody, and define the measurement of displacement and the velocity of the positioning point.
- (5) Define the measurement of time and the sensor to trigger the event when the position accuracy is met.
- (6) Select  $G_1$ ,  $G_2$ ,  $G_3$ , and  $G_4$  as design variables, define the total positioning time as the objective function, and use the global optimization method to get the optimal result.

By using the above variable motion boundary condition nonlinear dynamic-response optimization, the parameters likely to cause resonance will be excluded from the optimization of feasible solutions; thus, velocity planning is obtained in which the temporal distribution of inertial energy is optimal. Moreover, the presented velocity-planning meth-

od can also be applied to any other parameterized motion curves, as well as to the parameter optimization of control systems.

## 6 Numerical examples

Consider the structural optimization and velocity planning of a high-acceleration low-load die bonder for an integrated circuit (IC) packaging device, with a production rate of 36 000 dies per hour. The motion time for the bonder to move from the wafer to the lead frame (Figure 5) is only 50 ms. The external load is the inertial force of the die, which is negligible when compared with that of the die bonder.

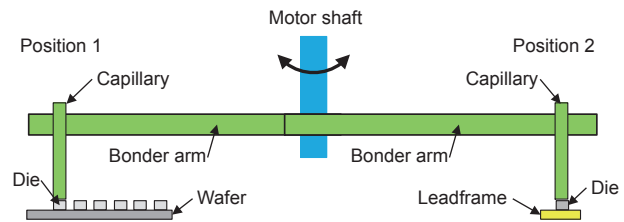


Figure 5. The working principle of the die bonder.

The material used is aluminum alloy 7075, with elastic modulus, mass density, and Poisson ratio of 79.9 GPa, 2700 kg·m<sup>-3</sup>, and 0.35, respectively. The radius of gyration is 80 mm, and the required positioning accuracy is ± 0.5 μm (after vibration attenuation). The size of the base structure is 105 mm × 30 mm × 5 mm, while the total mass is 0.3 kg, and the inertia property is 0.97 kg·mm<sup>2</sup>. The loads are the inertial force and the unit force applied to the tip of the capillary.

### 6.1 Optimal structural design

We have compared the structural optimization with three different methods, namely the traditional structural optimization, the ESLM with only one iteration in each cycle, and the modified ESLM. The nonlinear dynamic simulations of the optimal structures from the above methods are performed under the same motion profile with different parameters, where the motion period of the bonder is 100 ms (normal acceleration), 10 ms (high acceleration), and 1 ms (very high acceleration). The maximum amplitude of the residual vibrations is listed in Table 1. For the sake of comparison, the optimal structure using traditional structural optimization is set as the reference, and the vibration amplitude of the other two are compared with it. The results show that when the die bonder moves with a normal acceleration, the ESLM is nearly the same as the structural optimization (with a reduction of only 1.66%), and the data of the modified ESLM also gives similar results (with a decrease of only 3.09%). When the bonder arm moves with high acceleration, the ESLM is more efficient (dropping by 11.41%), and the modified ESLM with the vibration amplitude is reduced by 22.66%. It can be seen that the influence of inertial force is significant. When the bonder moves with very high acceleration, both the vibration amplitudes are very large, whilst the modified ESLM (21.11%) is still more efficient than the ESLM (less than 0.002%).

Table 1. Residual vibration of the capillary for different angular velocities [16].

Optimization method	Normal acceleration (motion time 100 ms)		High acceleration (motion time 10 ms)		Very high acceleration (motion time 1 ms)	
	Vibration amplitude (mm)	Improvement (%)	Vibration amplitude (mm)	Improvement (%)	Vibration amplitude (mm)	Improvement (%)
Traditional structural optimization	0.00421	—	0.0587	—	5.2688	—
ESLM(1 iteration)	0.00414	1.66	0.0520	11.41	5.2687	0.002
Modified ESLM	0.00408	3.09	0.0454	22.66	4.1565	21.11

Table 2. The iteration of nonlinear response optimization of the parameterized motion profile.

Iteration	$T_{1234}$ (ms)	$T_s$ (ms)	$G_1$ ( $^{\circ}\text{s}^{-3}$ )	$G_2$ ( $^{\circ}\text{s}^{-3}$ )	$G_3$ ( $^{\circ}\text{s}^{-3}$ )	$G_4$ ( $^{\circ}\text{s}^{-3}$ )
0	18.045	0.115	1.0000E+9	1.0000E+9	1.0000E+9	1.0000E+9
1	16.048	0.533	2.4312E+9	8.7876E+8	8.7876E+8	3.8280E+9
2	13.549	0.120	2.9124E+9	8.8347E+8	2.7710E+9	4.9866E+9
3	13.261	0.936	2.2908E+9	2.3951E+9	3.6078E+9	3.9223E+9
4	11.153	0.115	8.5732E+9	2.4061E+10	2.8029E+9	3.0347E+9

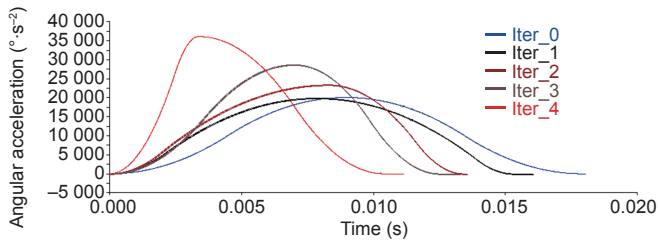


Figure 6. The angular acceleration during optimization.

6.2 Motion profile planning

Furthermore, the parameters of the motion profile have been optimized using the nonlinear response optimization (Figure 6), and after four iterations (Table 2), convergence was achieved.

In order to show the efficiency of the asymmetric S curve, the vibration response is compared with the symmetric S curve. If the let  $G_1 = G_2 = G_3 = G_4 = G$  in Eqs. (25)–(28), then the jerk of the symmetric S curve with an equivalent drive is the same, and both S curves being compared have the same driven time (Figure 7). We can see that the positioning time changes from 19.40 ms to 11.15 ms at positioning accuracy  $\pm 0.5 \mu\text{m}$ , a reduction of 42.5%.

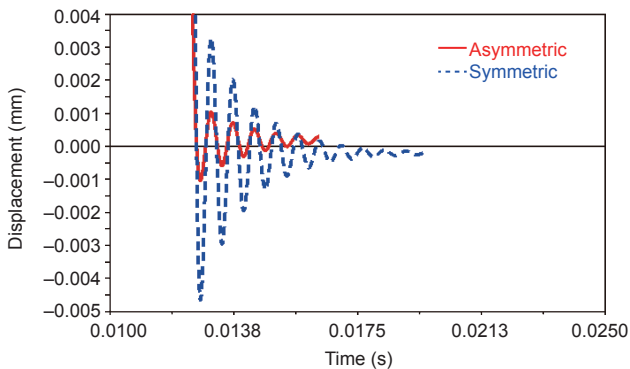


Figure 7. The residual vibration of asymmetric and symmetric S curves with the same driven time.

7 Engineering application

In order to show its practical significance in engineering, the presented method is applied to the development of a die bonder. The bonder is a swing arm that is directly driven by a servo moto. The original design is shown in Figure 8(a).

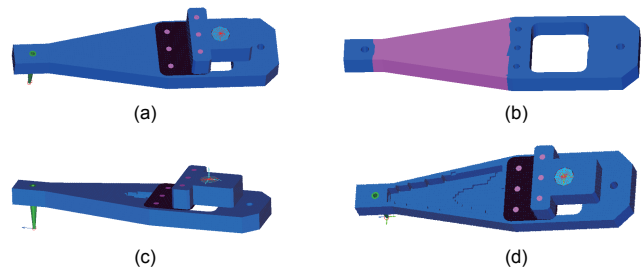


Figure 8. The structure of a die bonder. (a) Base structure; (b) design area; (c) optimal design; (d) final design.

7.1 Optimal structural design

The presented method is based on the finite element model, with 13 146 elements (6046 elements in the design domain). The material used is aluminum, with a Young’s modulus of 79 GPa, Poisson ratio of 0.33, and mass density of  $2700 \text{ kg}\cdot\text{m}^{-3}$ .

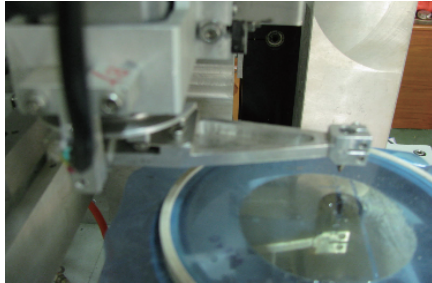
After four iterations, the optimal result was found by deleting 2000 elements (Figure 8(c)). The final design is shown in Figure 8(d). The vibration amplitude dropped by 94.00%, and the power consumption was also reduced by 38.46% (Table 3). The final design was selected as the engineering design (Figure 9).

7.2 Motion profile planning

In order to show the efficiency of the proposed motion profile based on the temporal optimal distribution of inertial energy, the same procedure is applied to the parameter optimization of a proportion-integration-differentiation (PID) control system (Figure 10).

**Table 3. Comparison of the vibration and power consumption.**

	Mass (g)	Vibration amplitude (mm)	Improvement (%)	Power (W)	Improvement (%)
Base	40.59	0.4014	—	21.496	—
Optimal	34.06	0.0291	92.75	16.722	22.21
Final	30.11	0.0241	94.00	13.229	38.46


**Figure 9. The engineering design.**

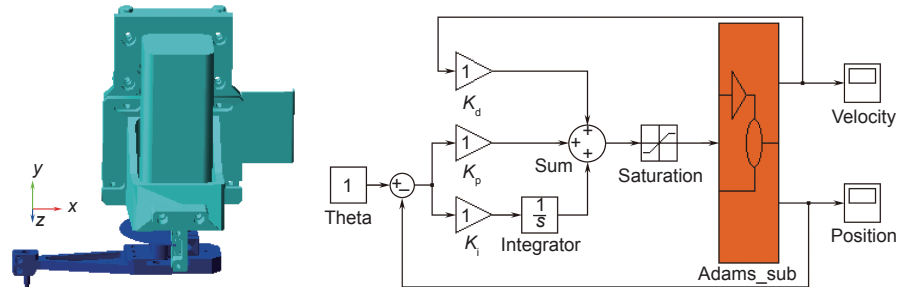
The initial values of the three variables  $K_p$ ,  $K_i$ , and  $K_d$  are set as 1.00. The original positioning time is 6.3215 s. Using parameter optimization based on nonlinear dynamic simulation using finite element analysis, after four iterations (Table 4), the optimal results are found with  $K_p$ ,  $K_i$ , and  $K_d$  at the values of 694.20, 14.225, and 340.41, respectively. This procedure also shows the efficiency of the two presented methods.

**Table 4. The optimization process of PID.**

Iteration number	Positioning time (s)	$K_p$	$K_i$	$K_d$
0	6.3215	1.00	1.00	1.00
1	2.4382	203.41	61.226	119.54
2	0.0905	587.71	56.752	110.80
3	0.0664	639.08	20.294	280.16
4	0.0594	694.20	14.225	340.41

## 8 Conclusions

In this paper, the optimization problem of the nonlinear dynamic response of a high-acceleration low-load mechanism was discussed. Systematic methods were proposed to solve the problem from the optimal distribution of inertial energy in space and time domains. A modified ESLM was selected for optimal structural design in order to improve the dynamic response of high-acceleration low-load mechanisms. A new velocity profile based on nonlinear dynamic response was proposed in order to reduce positioning time. The numerical example showed that the modified ESLM is efficient for high-


**Figure 10. The control model.**

acceleration low-load mechanisms and reduces the residual vibration by 20%; while the nonlinear dynamic response for the asymmetric S curve is decreased by more than 40%. The presented method was also applied to a design of a die bonder and to an optimal design of the PID parameters of a control system; both procedures showed the efficiency of the method. The method has also been tested on a variety of high-acceleration low-load mechanisms in IC packaging equipment design (such as die bonders, wire bonders, surface mount technology (SMT), and high-acceleration robotics, etc.), and a significant achievement has been accomplished.

## Acknowledgements

This work is supported by the National Key Basic Research Program of China (2011CB013104), National Natural Science Foundation of China (U1134004), Guangdong Provincial Natural Science Foundation (2015A030312008), Science and Technology Program of Guangzhou (201510010281), and Guangdong Provincial Science and Technology Plan (2013B010402014).

## Compliance with ethics guidelines

Xin Chen, Youdun Bai, Zhijun Yang, Jian Gao, and Gongfa Chen declare that they have no conflict of interest or financial conflicts to disclose.

## References

- H. Ding, L. M. Zhu, Z. Q. Lin. Accurate positioning and operation of high acceleration and high precision stage for IC packaging. *Prog. Nat. Sci.*, 2003, 13(6): 568–574 (in Chinese)
- Z. H. Feng, H. Y. Hu. Advances in dynamics of high-speed mechanisms. *Adv. Mech.*, 2002, 32(2): 196–204 (in Chinese)
- O. Wallrapp. Review of past developments in multibody system dynamics at DLR—From FADYNA to SIMPACK. *Vehicle Syst. Dyn.*, 2004, 41(5): 339–348
- W. S. Choi, G. J. Park. Structural optimization using equivalent static loads at all the time intervals. *Comput. Method. Appl. M.*, 2002, 191(19–20): 2105–2122
- G. J. Park, B. S. Kang. Validation of a structural optimization algorithm transforming dynamic loads into equivalent static loads. *J. Optimiz. Theory App.*, 2003, 118(1): 191–200
- W. S. Choi, G. J. Park. Structural optimization using equivalent static loads at all time intervals. *Comput. Method. Appl. M.*, 2002, 191(19–20): 2105–2122
- Y. I. Kim, G. J. Park. Nonlinear dynamic response structural optimization using equivalent static loads. *Comput. Method. Appl. M.*, 2010, 199(9–12): 660–676
- M. K. Shin, K. J. Park, G. J. Park. Optimization of structures with nonlinear behavior using equivalent loads. *Comput. Method. Appl. M.*, 2007, 196(4–6): 1154–1167

9. H. A. Lee, Y. I. Kim, G. J. Park, R. M. Kolonay, M. Blair, R. A. Canfield. Structural optimization of a joined wing using equivalent static loads. *J. Aircraft*, 2007, 44(4): 1302–1308
10. B. S. Kang, G. J. Park, J. S. Arora. Optimization of flexible multibody dynamic systems using the equivalent static load method. *AIAA J.*, 2005, 43(4): 846–852
11. K. D. Nguyen, T. C. Ng, I. M. Chen. On algorithms for planning S-curve motion profiles. *Int. J. Adv. Robot. Syst.*, 2008, 5(1): 99–106
12. K. Zheng, L. Cheng. Adaptive s-curve acceleration/deceleration control method. In: *Proceedings of the 7th World Congress on Intelligent Control and Automation*. Chongqing, China, 2008: 2752–2756
13. P. H. Meckl. Optimized s-curve motion profiles for minimum residual vibration. In: *Proceedings of the 1998 American Control Conference*. Philadelphia, PA, USA, 1998: 2627–2631
14. H. Z. Li, Z. Gong, W. Lin, T. Lippa. A new motion control approach for jerk and transient vibration suppression. In: *Proceedings of 2006 IEEE International Conference on Industrial Informatics*. Singapore, 2006: 676–681
15. Z. J. Yang. Topological optimization approach for structure design of high acceleration mechanisms using equivalent static loads method. *J. Mech. Eng.*, 2011, 47(17): 119–126 (in Chinese)
16. Z. J. Yang, X. Chen, R. Kelly. A topological optimization approach for structural design of a high-speed low-load mechanism using the equivalent static loads method. *Int. J. Numer. Meth. Eng.*, 2012, 89(5): 584–598
17. H. Li, M. D. Le, Z. M. Gong, W. Lin. Motion profile design to reduce residual vibration of high-speed positioning stages. *IEEE/ASME T. Mech.*, 2009, 14(2): 264–269